



ELSEVIER

Contents lists available at ScienceDirect

Physica B

journal homepage: [www.elsevier.com/locate/physb](http://www.elsevier.com/locate/physb)

# Mass-imbalanced Hubbard model in optical lattice with site-dependent interactions



Duc-Anh Le<sup>a,\*</sup>, Thi-Thu-Trang Tran<sup>a</sup>, Anh-Tuan Hoang<sup>b</sup>, Toan-Thang Nguyen<sup>b</sup>, Minh-Tien Tran<sup>c,d</sup>

<sup>a</sup> Faculty of Physics, Hanoi National University of Education, Xuan Thuy 136, Cau Giay, Hanoi 10000, Viet Nam

<sup>b</sup> Institute of Physics, PO Box 429, Bo Ho, Hanoi 10000, Viet Nam

<sup>c</sup> Institute of Research and Development, Duy Tan University, K7/25 Quang Trung, Danang, Viet Nam

<sup>d</sup> Institute of Physics, VAST, 10 Dao Tan, Ba Dinh, Hanoi 10000, Viet Nam

## ARTICLE INFO

### Keywords:

Mass-imbalance  
Hubbard model  
Optical lattice  
Mott transition  
Dynamical mean field theory

## ABSTRACT

We study the half-filled mass-imbalanced Hubbard model with spatially alternating interactions on an optical bipartite lattice by means of the dynamical mean-field theory. The Mott transition is investigated via the spin-dependent density of states and double occupancies. The phase diagrams for the homogeneous phases at zero temperature are constructed numerically. The boundary between metallic and insulating phases at zero temperature is analytically derived within the dynamical mean field theory using the equation of motion approach as the impurity solver. We found that the metallic region is reduced with increasing interaction anisotropy or mass imbalance. Our results are closely relevant to current researches in ultracold fermion experiments and can be verified through experimental observations.

## 1. Introduction

The Mott metal-insulator transition (MIT), a fundamental problem in condensed matter physics, is often studied within the Hubbard model (HM) [1] and its simplified version, the Falikov - Kimball model (FKM) [2]. These models describe itinerant electrons moving on a lattice and subjected to on-site repulsive interaction. When the on-site Coulomb interaction is strong enough, it essentially leads electrons to a localization, which yields the Mott insulating state. In condensed matter physics, the HM is just a simplified modeling of real materials. However, in real materials, the corresponding model parameters are hardly tuned in order to observe the MIT. With the achievement of laser cooling technique, optical lattices of ultracold neutral atoms can be established and they can simulate the HM [3,4]. The simulation of the HM allows us to easily control and tune the model parameters [5]. Actually, the MIT was observed in an optical lattice which simulates the HM [3,4]. The quantum simulations by the optical lattices not only allow us to experimentally explore the physical properties of the simulated models but they also can create novel model features. For instance, by varying the parameters of lasers being used, one can separately vary the hopping parameter of each spin component in the HM. As a result, this creates a mass imbalance between the spin components in the HM [6–12]. The mass imbalance strongly affects the

MIT. In particular, with mass imbalance, the lighter particles are more affected by correlations than the heavy ones and the critical interaction value of the MIT monotonically decreases with the growing of mass imbalance [13–18]. The HM with a mass imbalance is the natural connection between the HM and FKM. It is usually referred as the asymmetric Hubbard model (AHM) [19]. In addition to the mass imbalance, the quantum simulation of the HM also allows us to make a spatial modulation of the local interaction [20]. This gives rise to interest in studying the correlation effect of the site dependence of the local interaction [21–23]. The simplest form of the spatial modulation of the local interaction is an alternating of the local interaction in the lattice. In general, the local interaction can be repulsive or attractive at each sublattice sites. The repulsive interaction favors the antiferromagnetic state, while the attractive one favors the superfluid state. At half filling, due to the particle-hole symmetry, the repulsive and the attractive interactions are equivalent [21,22]. However, when the local interaction at the two penetrating sublattices has different signs, at half filling the antiferromagnetic and the superfluid states are not realized. Instead of these states, a MIT occurs [21,22]. It is interesting to study the effect of the mass imbalance on this MIT.

In this work, we study the Mott transition in the Hubbard model in the presence of both the mass imbalance and the spatial alternating of the local interaction by means of the dynamical mean-field theory

\* Corresponding author.

E-mail address: [anhld@hnue.edu.vn](mailto:anhld@hnue.edu.vn) (D.-A. Le).

(DMFT) [24]. The phase boundary between metallic and insulating phases at zero temperature is analytically derived within the dynamical mean field theory using the equation of motion approach as the impurity solver. We found that the metallic region is reduced with increasing interaction anisotropy or mass imbalance. We reveal the nature of the Mott states via the spin-dependent density of states (DOS) and the double occupancies for each sublattices as a function of the local interactions strengths. Our results are closely relevant to current researches in ultracold fermion experiments and can be verified through experimental observations [25,26].

The structure of the paper is as follows. In Section 2 we present the model and its dynamical mean-field theory. In Section 3 we present and discuss the numerical results of the ground state in paramagnetic states. Finally, the conclusions are presented in Section 4.

## 2. Model and its dynamical mean-field theory

We consider the following asymmetric Hubbard model with spatially modulated interaction on a bipartite lattice

$$H = - \sum_{\langle ij \rangle \sigma} t_\sigma [c_{i\sigma}^\dagger c_{j\sigma} + \text{H. c.}] - \sum_{i\sigma} \mu_\sigma n_{i\sigma} + \sum_{\alpha, i \in \alpha} U_\alpha \left( n_{i\uparrow} n_{i\downarrow} - \frac{1}{2} [n_{i\uparrow} + n_{i\downarrow}] \right), \quad (1)$$

where  $c_{i\sigma}$  ( $c_{i\sigma}^\dagger$ ) annihilates (creates) a fermion with spin  $\sigma$  at site  $i$ ,  $n_{i\sigma} = c_{i\sigma}^\dagger c_{i\sigma}$  and  $n_i = n_{i\uparrow} + n_{i\downarrow}$ . We denote  $A$  and  $B$  the two penetrating sublattices.  $U_\alpha$  is the site-dependent local interaction in the sublattice  $\alpha$  ( $\alpha = A, B$ ). Here, for simplicity we only consider the alternating interaction.  $t_\sigma$  is the nearest-neighbor hopping parameter for spin  $\sigma$  and  $\mu_\sigma$  is the chemical potential, which is chosen so that the average occupancy is 1 (half-filling). The mass imbalance is introduced via  $r = t_\uparrow/t_\downarrow$ . When  $r \neq 1$  the  $SU(2)$  symmetry in both the spin space and the time-reversal symmetry are broken. When  $U_A=U_B$  the model (1) is reduced to the asymmetric Hubbard model [13–18]. In the mass balanced case, i.e.  $r=1$ , the model under consideration is reduced to the typical Hubbard model with site-dependent interactions [21–23]. The model described by the Hamiltonian in Eq. (1) can be simulated by loading two-component fermionic atoms into an optical lattice [3,4].

We investigate the proposed model by using the DMFT. Within the DMFT the self energy is a local function of frequency. This approximation becomes exact in the limit of lattices with an infinite coordination. However, for lattices with finite coordinations, self energy is a local function of frequency is just an approximation. The self energy is self-consistently determined from a single impurity embedded in an effective medium. This single correlated impurity is described by the Anderson model

$$H_{\text{aimp}} = \sum_{k\sigma} \varepsilon_{ak\sigma} c_{k\sigma}^\dagger c_{k\sigma} - \sum_{\sigma} \mu_\sigma n_{d\sigma} + \sum_{k\sigma} (V_{ak\sigma} c_{k\sigma}^\dagger d_\sigma + V_{ak\sigma}^* d_\sigma^\dagger c_{k\sigma}) + U_\alpha \left( n_{d\uparrow} n_{d\downarrow} - \frac{1}{2} [n_{d\uparrow} + n_{d\downarrow}] \right), \quad (2)$$

where  $d_\sigma$  and  $d_\sigma^\dagger$  are the impurity operators with spin  $\sigma$  and  $\varepsilon_{ak\sigma}$  is the energy of conduction electrons hybridized with the impurity by  $V_{ak\sigma}$ . The effective parameters  $\varepsilon_{ak\sigma}$  and  $V_{ak\sigma}$  enter the hybridization function as

$$\Delta_{\alpha\sigma}(\omega) = \sum_k \frac{V_{ak\sigma}^2}{\omega - \varepsilon_{ak\sigma}}. \quad (3)$$

The impurity Green function is mapped onto the on-site Green function of the original lattice model in Eq. (1) by

$$G_{\alpha\sigma}(\omega) = G_{i\alpha\sigma}(\omega) = \int_{-\infty}^{+\infty} \frac{\xi_{\alpha\sigma}(\omega) \rho_\sigma^0(z) dz}{\xi_{\alpha\sigma}(\omega) \xi_{\alpha\sigma}(\omega) - z^2}, \quad (4)$$

where  $\xi_{\alpha\sigma}(\omega) = \omega + \mu_\sigma + \frac{U_\alpha}{2} - \Sigma_{\alpha\sigma}(\omega)$  with  $\Sigma_{\alpha\sigma}(\omega)$  is the local self-energy for the sublattice  $\alpha$ . For the Bethe lattice with an infinite coordination number

$$\rho_\sigma^0(z) = \frac{1}{2\pi t_\sigma^2} \sqrt{4t_\sigma^2 - z^2}, \quad (5)$$

and the self-consistent condition is given by

$$\Delta_{\alpha\sigma}(\omega) = t_\sigma^2 G_{\alpha\sigma}(\omega), \quad (6)$$

$$G_{0\alpha\sigma}^{-1}(\omega) = \omega + \mu_\sigma + \frac{U_\alpha}{2} - \Delta_{\alpha\sigma}(\omega). \quad (7)$$

Here  $G_{\alpha\sigma}(\omega)$  is the local Green function of the fermions with spin  $\sigma$  and  $G_{0\alpha\sigma}$  are the bare Green functions of the associated quantum impurity problem for the sublattices  $\alpha$ .

In order to calculate the Green function of the single impurity Anderson model we make use of the equation of motion method [27]. Decoupling the equations of motion of the single impurity Anderson model (2) to the second order, one yields the following approximation for the impurity Green function:

$$G_{\alpha\sigma}(\omega) = \frac{1 - n_{\alpha\bar{\sigma}}}{\omega + \mu_\sigma + U_\alpha/2 - \Delta_{\alpha\sigma} + \frac{U_\alpha \Pi_{1\alpha\sigma}(\omega)}{\omega + \mu_\sigma - U_\alpha/2 - \Delta_{\alpha\sigma} - \Pi_{3\alpha\sigma}(\omega)}} + \frac{n_{\alpha\bar{\sigma}}}{\omega + \mu_\sigma - U_\alpha/2 - \Delta_{\alpha\sigma} - \frac{U_\alpha \Pi_{2\alpha\sigma}(\omega)}{\omega + \mu_\sigma + U_\alpha/2 - \Delta_{\alpha\sigma} - \Pi_{3\alpha\sigma}(\omega)}}, \quad (8)$$

in which the function  $\Pi_{i\alpha\sigma}$  reads

$$\Pi_{i\alpha\sigma}(\omega) = \int_{-\infty}^{+\infty} dz \Gamma_{\alpha\bar{\sigma}}(z) \frac{F_i(z)}{\omega + \mu_\sigma - \mu_{\bar{\sigma}} - z} + \int_{-\infty}^{+\infty} dz \Gamma_{\alpha\bar{\sigma}}(z) \frac{F_i(z)}{\omega + \mu_\sigma + \mu_{\bar{\sigma}} + z}, \quad (9)$$

where  $F_1(z) = f(z)$ ,  $F_2(z) = 1 - f(z)$ ,  $F_3(z) = 1$ , with  $f(z) = (\exp(\frac{z}{T}) + 1)^{-1}$  being the Fermi distribution function;  $n_{\alpha\sigma} = \int dz f(z) \rho_{\alpha\sigma}(z)$  and  $\Gamma_{\alpha\sigma}(z) = -\frac{1}{\pi} \text{Im} \Delta_{\alpha\sigma}(z + i\eta)$ , where  $\eta$  is a positive infinitesimal number. Our study is restricted to the paramagnetic case at half-filling:  $\mu_\uparrow = \mu_\downarrow = 0$  and  $n_{\alpha\uparrow} = n_{\alpha\downarrow} = 1/2$ . Due to the particle-hole symmetry, it follows that

$$\Pi_{1\alpha\sigma}(\omega) = \Pi_{2\alpha\sigma}(\omega) = \frac{\Pi_{3\alpha\sigma}(\omega)}{2} = \Delta_{\alpha\bar{\sigma}}(\omega). \quad (10)$$

Inputting these conditions (10) into Eq. (8), one easily obtains

$$G_{\alpha\sigma}(\omega) = \frac{1}{2} \frac{1}{G_{0\alpha\sigma}^{-1}(\omega) + \frac{U_\alpha \Delta_{\alpha\bar{\sigma}}(\omega)}{G_{0\alpha\sigma}^{-1}(\omega) - U_\alpha - 2\Delta_{\alpha\bar{\sigma}}(\omega)}} + \frac{1}{2} \frac{1}{G_{0\alpha\sigma}^{-1}(\omega) - U_\alpha - \frac{U_\alpha \Delta_{\alpha\bar{\sigma}}(\omega)}{G_{0\alpha\sigma}^{-1}(\omega) - 2\Delta_{\alpha\bar{\sigma}}(\omega)}}. \quad (11)$$

Eqs. (4), (6), (7) and (11) form a closed set of algebraic equations for  $G_{\alpha\sigma}(\omega)$  ( $\sigma = \uparrow, \downarrow$ ;  $\alpha = A, B$ ). In homogeneous interaction system  $U_A=U_B$ , the Eqs. (11) reproduce the results in [16,17], which are exact in the Falikov-Kimball limit  $r=0$  and are known as the (full) Hubbard III approximation of the Hubbard model in the limit  $r=1$ .

In order to study the MIT in the system with alternating interactions, we calculate the spin-dependent DOSs for each sublattice  $\rho_{\alpha\sigma}(\omega) = -\mathcal{I} G_{\alpha\sigma}(\omega)/\pi$ , DOSs at the Fermi level  $\rho_{\alpha\sigma}(0)$  and double occupancy  $D_\alpha = \langle n_{\alpha\uparrow} n_{\alpha\downarrow} \rangle$ . We then construct the phase diagrams for the homogeneous phases at  $T = 0$  K.

### 3. Results and discussions

In this section, we present and discuss results of the self-consistent DMFT Eqs. (4), (6), (7) and (11). The systems of equations are solved numerically by simple iterations to determine the self-energy  $\Sigma_{\alpha\sigma}(\omega)$  and the Green function  $G_{\alpha\sigma}(\omega)$ . The algorithm is as follows: start with an initial self-energy guess  $\Sigma_{\alpha\sigma}(\omega)$ , we obtain the lattice Green function  $G_{\alpha\sigma}(\omega)$  from Eq. (4). Inputting the self-energy and the lattice Green function calculated in the previous step into Eqs. (6), (7) and (11), we can calculate a new Green function  $G_{\alpha\sigma}(\omega)$ . Finally, a new self-energy  $\Sigma_{\alpha\sigma}(\omega)$  is determined by using the Dyson equation

$$\Sigma_{\alpha\sigma}(\omega) = G_{0\alpha\sigma}^{-1}(\omega) - G_{\alpha\sigma}^{-1}(\omega). \quad (12)$$

This procedure is iterated until convergence is reached. In actual numerical calculations, we replace the real frequency by the complex one  $\omega \rightarrow \omega + i\eta$ , where  $\eta$  is a positive infinitesimal number. If  $\eta$  is too small the convergence is never reached. Thus,  $\eta$  must take a finite small value (should be in range from  $10^{-3}$  to  $10^{-2}$ ) to make the iterations converge. After that, we use the spline extrapolation to reach the limit  $\eta \rightarrow 0$  to get sharp pictures for the density of states, which is important to determine the critical value of the local interactions for the metal-insulator transition. In the mass balanced case, it has been reported that the groundstate is magnetically ordered in the repulsive model ( $U_a > 0$ ) whereas the superfluid state is stabilized in the attractive model ( $U_a < 0$ ) [22]. Restricting our discussion to the paramagnetic sector, in the following we focus on the case with the signs of interactions are different from each other ( $U_A U_B < 0$ ). Due to the particle-hole symmetry as mentioned earlier, we can assume that  $U_A > 0, U_B < 0$ . Hereafter, we set  $U_A = U > 0$  and  $U_B = -U/\gamma$  with  $\gamma > 0$  (called spatial modulation parameter). Under this condition, a paramagnetic groundstate is expected and a Mott metal-insulator transition is possible when the interactions are turned on and gradually increasing. We set  $D = 2t_1$  as the energy unit and  $r = t_1/t_2$ , which goes from the Falikov-Kimball limit  $r=0$  to the symmetric case  $r=1$ , as the mass imbalanced parameter.

First, in order to show how the mass imbalance affects the stability of the normal metallic states, we plot the spin-dependent density of states for each sublattice with  $U = 1.5D$  and  $\gamma = 0.8$  for different values of  $r$  in Fig. 1. We plotted the density of states of a metallic state, a state right at the MIT, and an insulating state. Here, the symmetry of the DOS reflects particle-hole symmetry in the half-filled system. When  $r=1.0$ , the DOSs for both spin species in the sublattices A and B at the

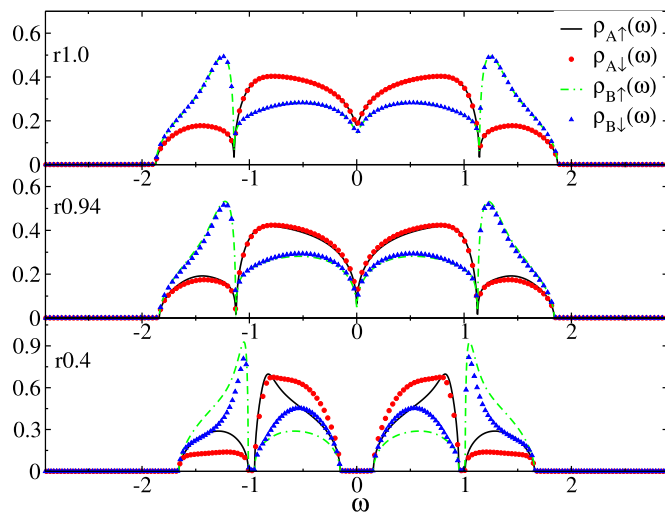


**Fig. 1.** Spin-dependent density of states for the sublattices for  $U = 1.5D$ , spatial modulation parameter  $\gamma = 0.8$  and various values of the mass imbalanced parameter  $r$ . Top panel: a metallic state for  $r=1.0$ ; Middle panel: MIT occurs at  $r_c=0.94$ ; Bottom panel: an insulator state for  $r=0.4$  (the half bandwidth with spin up  $D = 2t_1 = 1$ ).

Fermi level ( $\omega = 0$ ) are nonzero, which indicates that system is in a metallic state. In contrast, when  $r=0.4$ , the DOSs for both spin species in the sublattices A and B at the Fermi level show a gap around  $\omega = 0$ , indicating an insulating phase. The Mott transition in the system occurs at  $r_c=0.94$ . Because the DOSs at the Fermi level indicates the conduction properties of the system, we calculate these values and show them in Fig. 2. One can see that both  $\rho_{\alpha\sigma}(0)$  simultaneously vanish at the Mott transition. We note that because of the continuous nature of the transition, identifying the precise value of the critical asymmetric parameter is difficult. In the case of  $\gamma = 1.0, 0.9$ , and  $0.8$  by using a simple spline extrapolation from the data in the metallic phase we obtain  $r_c=0.73, 0.83$ , and  $0.94$  respectively. It means that, when  $U$  is fixed, the smaller spatial modulation parameter  $\gamma$ , the easier the mass imbalanced system is driven from a metallic state to the Mott phase.

Then, we discuss how the spatial modulation in the interactions affects the stability of the normal metallic states. In Fig. 3, we plot the spin-dependent density of states for each sublattice with  $U = 1.5D$  and  $r=0.8$  for different values of  $\gamma$ . We plotted the density of states of a metallic state, a state right at the MIT, and an insulating state. The particle-hole symmetry in the half-filled system is clearly seen. When

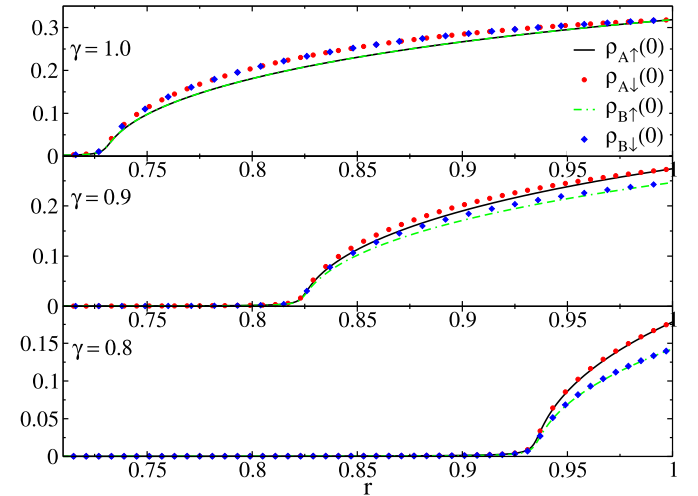


**Fig. 2.** DOSs at the Fermi level as a function of the mass imbalanced parameter  $r$  for  $U = 1.5D$  and various values of the spatial modulation parameter  $\gamma$ .

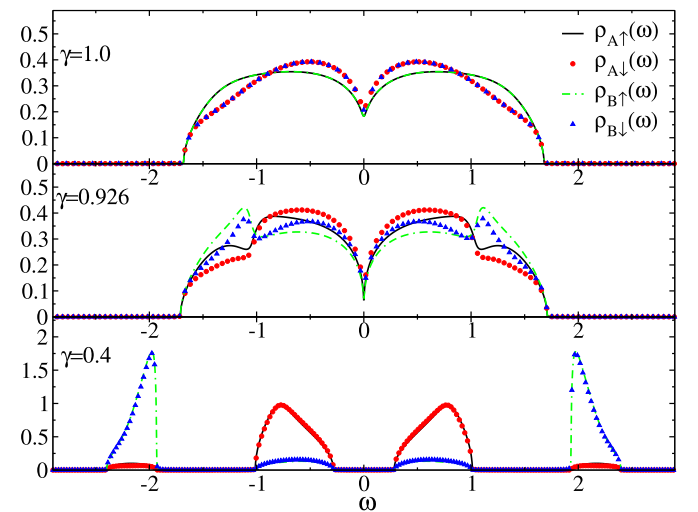


**Fig. 3.** Spin-dependent density of states for the sublattices for  $U = 1.5D$ ,  $r=0.8$  and various values of the spatial modulation parameter  $\gamma$ . Top panel: a metallic state for  $r=1.0$ ; Middle panel: MIT occurs at  $r_c = 0.926$ ; Bottom panel: an insulator state for  $r=0.4$  (the half bandwidth with spin up  $D = 2t_1 = 1$ ).

$\gamma = 1.0$ , the DOSs for both spin species in the sublattices A and B at the Fermi level ( $\omega = 0$ ) are finite, which indicates that system is metallic. In contrast, when  $\gamma = 0.4$ , the DOSs for both spin species in the sublattices A and B at the Fermi level show a gap around  $\omega = 0$ , indicating an insulating phase. The Mott transition in the system occurs at  $\gamma_C = 0.926$ . In order to find the critical value of the spatial modulation parameter  $\gamma_C$ , we show the DOSs at the Fermi level as a function of the spatial modulation parameter  $\gamma$  for  $U = 1.5D$  and various values of  $r$  in Fig. 4. One can see that both  $\rho_{\alpha\sigma}(0)$  simultaneously vanish at the Mott transition. In the case of  $r=1.0, 0.9$ , and  $0.8$  by using a simple spline extrapolation from the data in the metallic phase we obtain  $\gamma_C = 0.75, 0.83$ , and  $0.926$  respectively. It means that, when  $U$  is fixed, the smaller mass-imbalanced parameter  $r$ , the more symmetric interaction must be to drive the system from a metallic state to the Mott phase. Similar to the mass balanced case [21,22], the Mott transition at zero temperature in the mass-imbalanced system is continuous.

Next, in order to establish a link between the behavior of the model and the physical observable accessible in cold atom systems on optical lattices, we calculate the double occupation  $\langle n_{\uparrow}n_{\downarrow} \rangle$ . The numerical results are plotted in Fig. 5 for  $\gamma = 0.5$  and various values of  $r$ . As in Ref. [14], in the noninteracting case ( $U=0$ ), the double occupation is 0.25,

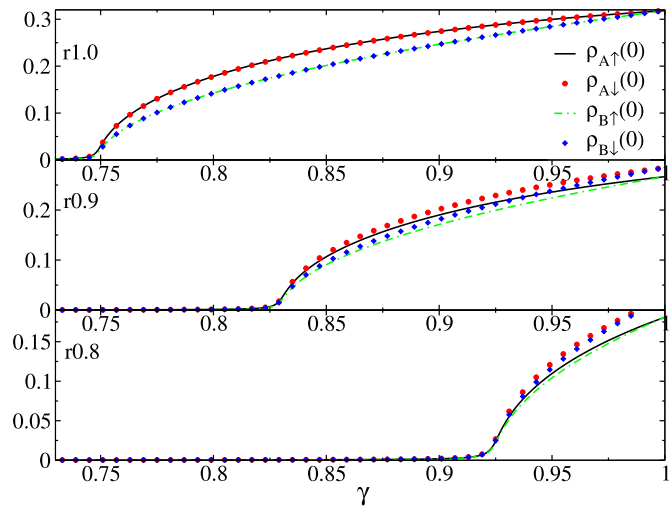


Fig. 4. Spin-dependent density of states at the Fermi level as a function of the mass imbalanced parameter  $r$  for  $U = 1.5D$  and various values of the spatial modulation parameter  $\gamma$ .

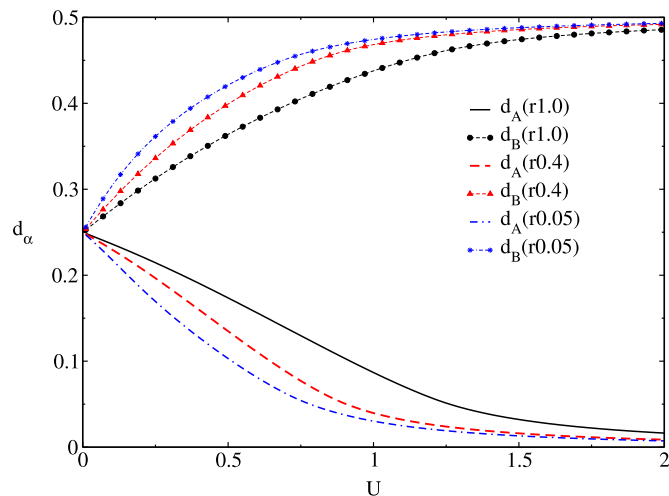


Fig. 5. Double occupation  $\langle n_{\uparrow}n_{\downarrow} \rangle$  as a function of  $U$  for  $\gamma = 0.5$  and different fixed values of  $r$ .

and it quickly decreases when  $U$  increases. A metal is characterized by a linear decrease in the double occupation with increasing interaction  $U$  while in the insulating region, at a larger value of the interaction, the double occupation remains small and weakly depends on  $U$ . As one might expect, at smaller values of  $r$ , the double occupation more rapidly decreases, and the value of the critical interaction is reduced.

We now present the critical spatial modulation interaction  $\gamma_C(r, U)$  for the half-filled model as a function of the mass imbalanced parameter  $r$  for different values of local interaction  $U = 1.0D, 1.5D$  and  $2.0D$  in Fig. 6. The more  $U$  increases, the more the metallic region is reduced as a results of strong correlation. In the Falikov-Kimball limit  $r=0$ , it is seen that  $\gamma_C(r = 0, U)$  equals to  $U^2$ . This relation holds for any values of  $U$ . When  $\gamma \rightarrow 0$ , i.e. the interaction in the B-sublattice is infinitely negative, there is no doubly occupancied state in the A-sublattice and there is no singly occupancied states in the B-sublattice. In the latter the empty state and the doubly occupancied state are randomly distributed with a probability of 1/2, whereas in the former the spin  $\uparrow$  state and the spin  $\downarrow$  state are randomly distributed with a probability of 1/2. Therefore, in the  $\gamma \rightarrow 0$  limit the system is insulating for whatever values of the mass imbalanced parameter  $r$ , i.e. the transition line  $\gamma_C(r, U)$  never crosses the horizontal axis.

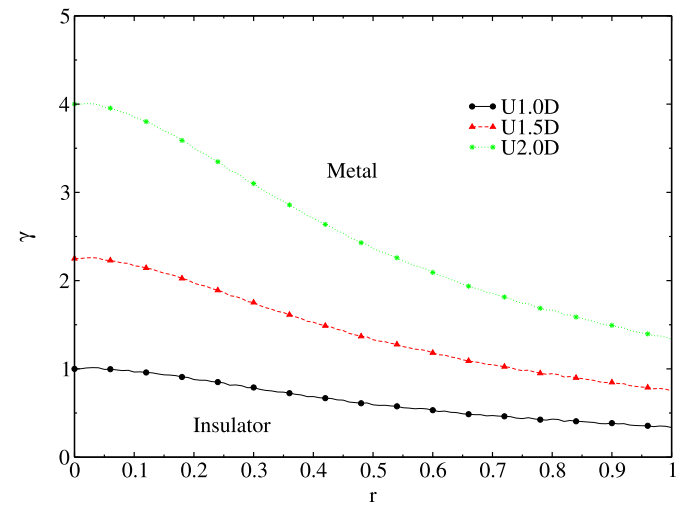


Fig. 6. The critical spatial modulation interaction  $\gamma_C$  for the half-filled model as a function of the mass imbalanced parameter  $r$  for different values of local interaction  $U = 1.0D, 1.5D$  and  $2.0D$ .

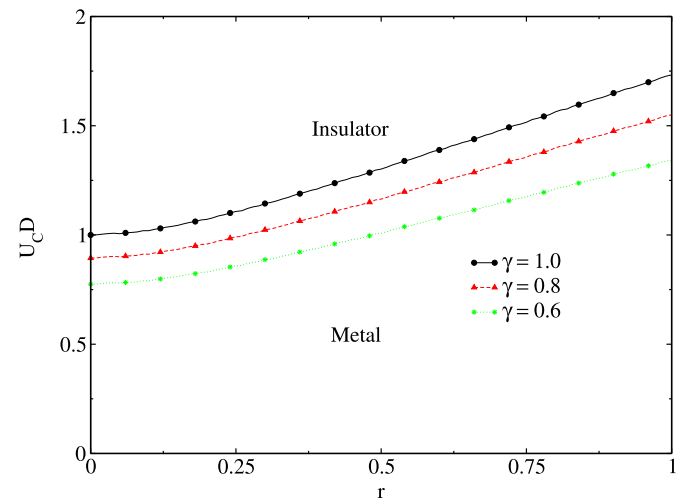


Fig. 7. The critical interaction  $U_C$  for the half-filled model as a function of the mass imbalanced parameter  $r$  for different values of spatial modulation interaction  $\gamma = 1.0, 0.8$  and  $0.6$ .

In Fig. 7, we show the critical interaction  $U_C$  for the half-filled model as a function of the mass imbalanced parameter  $r$  for different values of spatial modulation interaction  $\gamma = 1.0, 0.8$  and  $0.6$ . For homogeneous interactions, we reproduce results in Ref. [16,17] where  $U_C = [2(t_1^2 + t_1^2 + \sqrt{t_1^4 + t_1^4 + 14t_1^2 t_1^2})]^{1/2}$ . In the Falikov-Kimball limit  $r=0$ ,  $U_C(r=0, \gamma)$  equals to  $\sqrt{\gamma}$ . It is seen that the dependent of  $U_C(r, \gamma)$  on  $r$  for different fixed values of  $\gamma$  are similar. At fixed  $\gamma$ , the critical value for the Mott transition increases monotonically with increasing  $r$ . We found that the metallic region is reduced with increasing interaction anisotropy (decreasing  $\gamma$ ).

The above results are summarized into the phase diagram in Fig. 8. For the mass balanced case ( $r=1$ ), our results are in good agreement with those obtained from DMFT with NGR method [22]. In addition, the more asymmetric the system ( $r = \frac{t_1}{t_2}$  decreases), the more the metallic region reduces. It is easily understood since at fixed  $D$  or  $t_1$ , the more asymmetric the system, the stronger different the bare mass of the two component, the easier it is to localize the system.

Within the dynamical mean field theory, the critical value of the Mott transition in the half-filled mass-imbalanced Hubbard model with site-dependent interactions can be obtained analytically by using the equation of motion approach as the impurity solver. From Eqs. (11), at the Fermi level  $\omega = 0$ , one has

$$G_{A1} = -\frac{4(2G_{B1}t_1^2 + G_{B1}t_1^2)}{8G_{B1}G_{B1}t_1^2 t_1^2 + 4G_{B1}^2 t_1^4 - U_A^2}, \quad (13)$$

$$G_{A1} = -\frac{4(G_{B1}t_1^2 + 2G_{B1}t_1^2)}{4G_{B1}^2 t_1^4 + 8G_{B1}G_{B1}t_1^2 t_1^2 - U_A^2}, \quad (14)$$

$$G_{B1} = -\frac{4(2G_{A1}t_1^2 + G_{A1}t_1^2)}{8G_{A1}G_{A1}t_1^2 t_1^2 + 4G_{A1}^2 t_1^4 - U_B^2}, \quad (15)$$

$$G_{B1} = -\frac{4(G_{A1}t_1^2 + 2G_{A1}t_1^2)}{4G_{A1}^2 t_1^4 + 8G_{A1}G_{A1}t_1^2 t_1^2 - U_B^2}. \quad (16)$$

Due to the particle-hole symmetry, it follows that  $G_{\alpha\sigma}(0)$  are pure imaginary at the Fermi level  $\omega = 0$ , i.e.  $G_{\alpha\sigma}(0) = -i\rho_{\alpha\sigma}(0)$ . The metallic state ceases to exist when the density of states at the Fermi level  $\rho_{\alpha\sigma}(0) \rightarrow 0$  as  $U_\alpha \rightarrow U_{\alpha c}$ . By neglecting second order terms in (13)–(16), we end up with a set of linear homogeneous equations for  $\rho_{\alpha\sigma}(0)$  that has a non-trivial solution if and only if

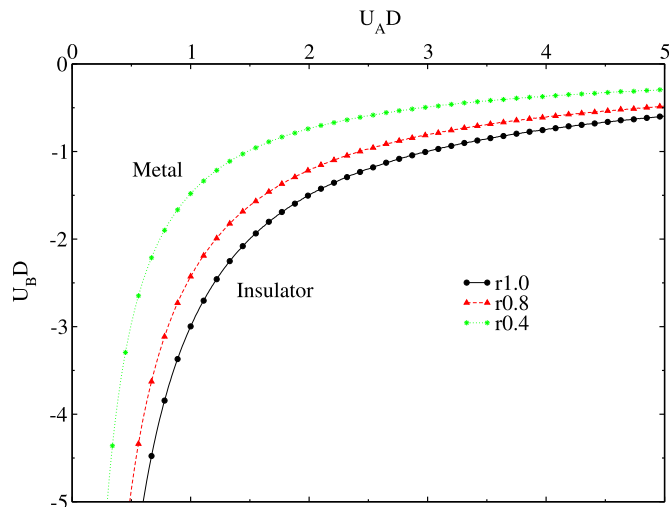


Fig. 8. Ground state phase diagram for the half-filled model as a function of the interactions  $U_A/D$  and  $U_B/D$  for different values of  $r = 1.0, 0.8$  and  $0.4$ .

$$\text{Det} \begin{vmatrix} 1 & 0 & -\frac{4t_1^2}{U_A^2} & -\frac{8t_1^2}{U_A^2} \\ 0 & 1 & -\frac{8t_1^2}{U_A^2} & -\frac{4t_1^2}{U_A^2} \\ -\frac{4t_1^2}{U_B^2} & -\frac{8t_1^2}{U_B^2} & 1 & 0 \\ -\frac{8t_1^2}{U_B^2} & -\frac{4t_1^2}{U_B^2} & 0 & 1 \end{vmatrix} = 0. \quad (17)$$

The above expression for the critical values is equivalent with

$$|U_A U_B| = 2(t_1^2 + t_1^2 + \sqrt{t_1^4 + t_1^4 + 14t_1^2 t_1^2}). \quad (18)$$

The expression (18) is our main result. In the case of the usual asymmetric Hubbard model  $U_A=U_B$ , we reproduce results in Ref. [16,17]. The condition for the existence of the metallic state (17) shows that the metallic state in the two sublattices must appear and disappear at the same time, i.e. only a single Mott transition occurs when two kind of interactions with different spin are switched on and gradually increases. As in the mass balanced case [21,22] the Mott transition at zero temperature in the mass-imbalanced system is continuous. This is basically the same as the transition between a band insulator and a correlated normal metal, which falls into the  $I-2 \rightarrow M-4$  universality class [28].

#### 4. Conclusions

In summary, we have used the equation of motion approach as an impurity solver for the dynamical mean field theory to investigate the Mott metal-insulator transition in the asymmetric Hubbard model with site-dependent interactions at half-filling and zero temperature. The technique has been implemented directly on the real-frequency axis, which turns out to be computationally efficient. In addition, it allows an explicit expression for the critical interaction in the system to be obtained as a function of model parameters. We also numerically computed the spin-dependent density of states at the Fermi level and the double occupation that may permit the experimental identification of this remarkable physical behavior. We clarify how mass imbalance and the spatial modulated interaction affect the stability of the normal metallic state. Similar to the mass balanced case, the Mott transition at zero temperature in the mass-imbalanced system is continuous. Our results here are closely relevant to current researches in ultracold fermion experiments and can be verified through experimental observations. With a suitable decoupling scheme, this approach can also be applied to the asymmetric Hubbard model with site-dependent interactions at half-filling for charge and spin orders. This is left to a future work.

#### Acknowledgments

This research is funded by Vietnam National Foundation for Science and Technology Development (NAFOSTED) under grant number 103.01-2015.21.

#### References

- [1] J. Hubbard, Proc. R. Soc. Lond. A 276 (1963) 238.
- [2] L.M. Falicov, J.C. Kimball, Phys. Rev. Lett. 22 (1969) 997.
- [3] R. Jördens, N. Strohmaier, K. Günter, H. Moritz, I. Esslinger, Nature 455 (2008) 204.
- [4] U. Schneider, L. Hackermüller, S. Will, T. Best, I. Bloch, T.A. Costi, R.W. Helmes, D. Rasch, A. Rosch, Science 322 (2008) 1520.
- [5] D. Jaksch, P. Zoller, Ann. Phys. 315 (2005) 52.
- [6] M. Tagliabier, A.-C. Voigt, T. Aoki, T.W. Hansch, K. Dieckmann, Phys. Rev. Lett. 100 (2008) 010401.
- [7] F.M. Spiegelhalder, A. Trenkwalder, D. Naik, G. Hendl, F. Schreck, R. Grimm, Phys. Rev. Lett. 103 (2009) 223203.
- [8] T.G. Tiecke, M.R. Goosen, A. Ludewig, S.D. Gensemer, S. Kraft, S.J.J.M.F. Kokkelmans, J.T.M. Walraven, Phys. Rev. Lett. 104 (2010) 053202.
- [9] S. Taie, Y. Takasu, S. Sugawa, R. Yamazaki, T. Tsujimoto, R. Murakami,

- Y. Takahashi, Phys. Rev. Lett. 105 (2010) 190401.
- [10] A. Trenkwalder, C. Kohstall, M. Zaccanti, D. Naik, A.I. Sidorov, F. Schreck, R. Grimm, Phys. Rev. Lett. 106 (2011) 115304.
- [11] C. Kohstall, M. Zaccanti, M. Jag, A. Trenkwalder, P. Massignan, G.M. Bruun, F. Schreck, R. Grimm, Nat. (Lond.) 485 (2013) 615.
- [12] M. Jag, M. Zaccanti, M. Cetina, R.S. Lous, F. Schreck, R. Grimm, D.S. Petrov, J. Levinsen, Phys. Rev. Lett. 112 (2014) 075302.
- [13] T.-L. Dao, M. Ferrero, P.S. Cornaglia, M. Capone, Phys. Rev. A 85 (2012) 013606.
- [14] E.A. Winograd, R. Chitra, M.J. Rozenberg, Phys. Rev. B 84 (2011) 233102.
- [15] E.A. Winograd, R. Chitra, M.J. Rozenberg, Phys. Rev. B 86 (2012) 195118.
- [16] I.V. Stasyuk, O.B. Hera, Eur. Phys. J. B 48 (2005) 339.
- [17] A.-T. Hoang, T.-T.-T. Tran, D.-A. Le, J. Kor. Phys. Soc. 68 (2016) 238.
- [18] A.-T. Hoang, D.-A. Le, Phys. B 485 (2016) 121.
- [19] D. Ueltschi, J. Stat. Phys. 116 (2004) 681.
- [20] R. Yamazaki, et al., Phys. Rev. Lett. 105 (2010) 050405.
- [21] T. Saitou et al., J. Supercond. Nov. Magn. 26, 1771, 2013,
- [22] A. Koga, et al., J. Phys. Soc. Jpn. 82 (2013) 024401.
- [23] D.-A. Le, T.-T.-T. Tran, A.-T. Hoang, Eur. Phys. J. B 86 (2013) 503.
- [24] A. Georges, et al., Rev. Mod. Phys. 68 (1996) 13.
- [25] G. Jotzu, M. Messer, F. Gorg, D. Greif, R. Desbuquois, T. Esslinger, Phys. Rev. Lett. 115 (2015) 073002.
- [26] D. Greif, T. Uehlinger, G. Jotzu, L. Tarruell, T. Esslinger, Science 340 (2013) 1307.
- [27] Y. Meir, N.S. Wingreen, P.A. Lee, Phys. Rev. Lett. 66 (1991) 3048.
- [28] M. Imada, A. Fujimori, Y. Tokura, Rev. Mod. Phys. 70 (1998) 1039.